Valence-sensitive determination of Cr^{3+} and Ce^{3+} concentration in doped $Sr_{0.61}Ba_{0.39}Nb_2O_6$ from magnetization studies and paramagnetic relaxation of Ce^{3+}

D. Schaniel,* Th. Woike, and G. Weckwerth
Institut für Mineralogie, Universität zu Köln, Zülpicherstr. 49b, 50674 Köln, Germany

J. Schefer
Laboratory for Neutron Scattering, ETH Zürich and PSI Villigen, 5232 Villigen PSI, Switzerland

M. Imlau, M. Wöhlecke, and R. Pankrath
Fachbereich Physik, Universität Osnabrück, 59069 Osnabrück, Germany
(Received 27 April 2004; revised manuscript received 21 June 2004; published 20 October 2004)

Magnetization- and susceptibility measurements are used as a method to determine the number density of the photorefractive centers Ce^{3+} and Cr^{3+} in $Sr_{0.61}Ba_{0.39}Nb_2O_6$ (SBN61). The number densities $\overline{n}_{Ce^{3+}} = 0.73(1) \cdot 10^{20}$ cm^{-3} and $\overline{n}_{Cr^{3+}} = 1.58(8) \cdot 10^{20}$ cm^{-3} were determined for crystals doped with 1.6 wt.% Ce and 20000 ppm Cr, respectively. Frequency dependent susceptibility measurements in the temperature range 3–10 K on SBN61: Ce show that the spin-lattice relaxation in this compound is dominated by the Orbach process. The crystal field splitting of the two lowest ground state doublets is determined to 1.77 meV. The susceptibility of SBN61: Cr shows no frequency dependence in the range 10–10^4 Hz.

DOI: 10.1103/PhysRevB.70.144410 PACS number(s): 75.20.Ck, 75.30.Cr, 81.70.Ex, 77.84.Dy

I. INTRODUCTION

Strontium barium niobate (SBN), $Sr_xBa_{1-x}Nb_2O_6$ ($0.25 \leqslant x \leqslant 0.75$), is a photorefractive material utilizable in a variety of optical applications, such as optical data storage,[1] data processing,[2] and optical phase conjugation.[3] These applications are based on the high photorefractive sensitivity and the large electro-optic coefficient r_{33}.[4] The average structure of the congruently melted $Sr_{0.61}Ba_{0.39}Nb_2O_6$ (SBN61), space-group $P4bm$, is a three-dimensional network of NbO_6 octahedra linked by their corners forming alternating five- and four-membered rings.[5] Five Sr and Ba atoms are distributed over six sites, where the Sr atoms occupy positions of symmetry 4 inside the square-shaped channels and all the Ba and some of the Sr atoms are located in the larger pentagonal channels, which are not fully occupied. This structure is a suitable host lattice for a variety of dopants such as rare earths and intermetallic elements, e.g., cerium, which is incorporated on a Sr^{2+} position,[6,7] or chromium, incorporated on a Nb^{5+}-position.[8] The doping with rare earths for example enhances the photorefractive properties[9] and is therefore used to tune the physical properties of SBN crystals used in optical applications. We investigated magnetic properties of SBN61 doped with Cr^{3+} and Ce^{3+}, in order to determine the concentration of these paramagnetic ions from the magnetization, as has recently been demonstrated by Dutta and co-workers[10] for Ni in NiSAPO catalysts. Hence the magnetization measurements are used as a method to determine the concentration of paramagnetic dopants besides the well established methods like electron paramagnetic resonance (EPR), Mössbauer spectroscopy, and photoemission, which are also sensitive to the valence state of the dopants. We have to stress that this method works only as long as interactions between the paramagnetic ions can be neglected, i.e., for low doping concentrations. The knowledge of the doping concentration of charge carriers is of importance for all phenomena depending on photoinduced charge transports, especially for holography, since e.g., the ratio of Ce^{3+}/Ce^{4+} ions determines the photorefractive properties of the material.[11]

II. EXPERIMENTAL DETAILS

The congruent SBN61 crystals doped with different amounts of Ce or Cr in the melt were grown by the Czochralski method in the crystal growth laboratory of the University of Osnabrück. The density of the samples was determined by the flotation method using a quartz single crystal ($\rho = 2.6481(3)$g cm^{-3}) for the calibration of the used liquids (paraffin oil, distilled water, and a zinc-bromide solution). The SBN61 crystal doped with 1.6 wt.% Ce has a density of $\rho = 5.3048(3)$g cm^{-3}. The number of Ce atoms per cubic centimeter $n_{Ce} = 1.92(8) \cdot 10^{20}$ cm^{-3} was determined by Instrumental Neutron Activation Analysis (INAA) in the same manner as described in detail in Ref. 6. SBN61 doped with 20000 ppm Cr has a density of $\rho = 5.290(1)$g cm^{-3} and $n_{Cr} = 1.64(8) \cdot 10^{20}$ cm^{-3}.[8] The magnetic measurements were performed on a Physical Properties Measurement System (PPMS) of Quantum Design, using the extraction method. The dc magnetization was measured in the temperature range 1.8–300 K with magnetic field strengths up to 9 Tesla, whereas the ac measurements were performed in the temperature range 1.8–10 K with external fields up to 0.2 Tesla. The amplitude of the driving ac field was chosen between 1 Oe and 10 Oe and frequencies ranging from 10 to 10^4 Hz. The sample mass was 487.9 mg for SBN61: Ce and 252.4 mg for SBN61:Cr. The magnetic field was applied perpendicular to the c-axis. For the SBN61: Ce crystal the angle between field direction and the a- or b-axis was about 5° (determined from the morphology).

III. PARAMAGNETIC RELAXATION

The magnetization in a paramagnetic substance (for N moles) is given by

$$M = NN_A g\mu_B J B_J(\eta), \tag{1}$$

where N_A is Avogadro's number, g is the effective g-value, μ_B is the Bohr magneton, J is the total angular momentum, B_J is the Brillouin function, and

$$\eta = \frac{g\mu_B J H_z}{k_B T}. \tag{2}$$

In the case $\eta \gg 1$ $B_J = 1$ one finds the saturation moment $M = N\, N_A g\mu_B J$. For $\eta \ll 1$ and using $M = \chi H_z$ one obtains the well known Curie law for paramagnets

$$\chi = \frac{N\, N_A g^2 \mu_B^2 J(J+1)}{3k_B T} = \frac{NC}{T} \tag{3}$$

with $C = 0.125 g^2 J(J+1)$ cm^3 K mol^{-1} the Curie constant.

After excitation such an assembly of isolated magnetic ions relaxes into thermal equilibrium via different spin-lattice relaxation processes. The three main relaxation processes determining the relaxation time τ are the direct, the Raman, and the Orbach process. For a Kramers ion with an isolated doublet (energy difference between the lowest doublets larger than $k_B T$) one obtains for the relaxation time τ,[12]

$$\frac{1}{\tau} = A_2 H^4 T + B_2 T^9 + C_2 e^{-(\Delta'/k_B T)} \tag{4}$$

where A_2, B_2, and C_2 are constants characteristic for the corresponding direct, Raman, and Orbach process, respectively, and Δ' is the energetic separation to the next doublet. The response of such a system to an applied oscillating magnetic field (frequency ω) is given by the Debye equation[12,13]

$$\chi(\omega) = \frac{\chi_T - \chi_{\mathrm{ad}}}{1 + i\omega\tau} + \chi_{\mathrm{ad}}, \tag{5}$$

where χ_T is the isothermal (low frequency limit, i.e., $\omega\tau \ll 1$) and χ_{ad} the adiabatic ($\omega\tau \gg 1$) susceptibility. Equation (5) gives an adequate description of the frequency dependence of the dynamic susceptibility as long as it is possible to characterize the spin-lattice relaxation process with a single relaxation time τ. If there is more than one time constant present in the investigated system, one uses the Cole-Cole formalism[14] to describe the frequency dependence of $\chi(\omega)$. The Cole-Cole formalism involves a modeling of the dynamics at a given temperature with a distribution of relaxation times that is symmetric on a logarithmic time scale. In this formalism Eq. (5) is modified to

$$\chi(\omega) = \frac{\chi_T - \chi_{\mathrm{ad}}}{1 + (i\omega\tau_c)^{1-\alpha}} + \chi_{\mathrm{ad}}, \tag{6}$$

where τ_c is the mean relaxation time. The parameter α determines the width of the distribution, such that $\alpha = 1$ corresponds to an infinitely wide distribution, while for $\alpha = 0$ the Cole-Cole equation [Eq. (6)] reduces to the Debye equation [Eq. (5)] with a single relaxation time. The Cole-Cole equation may be decomposed into its real (χ') and imaginary (χ'') part

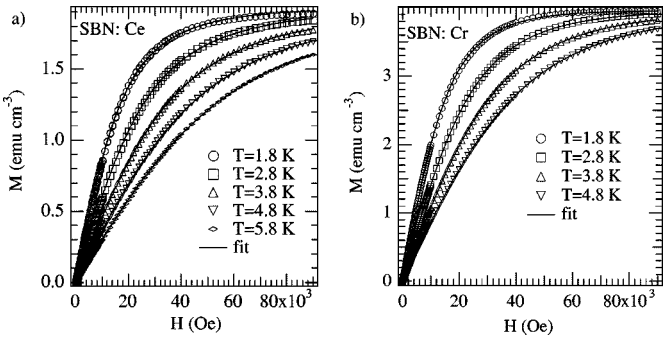

FIG. 1. (a) $M(H)$ for SBN61: Ce. The fit yields $N_{Ce^{3+}} = 1.19(1)\cdot 10^{-4}$ mol$\cdot$cm^{-3} and $g = 1.16(1)$ (b) $M(H)$ for SBN61: Cr. $N_{Cr^{3+}} = 2.51(6)\cdot 10^{-4}$ mol$\cdot$cm^{-3}, $g = 1.88(2)$.

$$\chi'(\omega) = \chi_{\mathrm{ad}} + \frac{\chi_T - \chi_{\mathrm{ad}}}{2}\left(1 - \frac{\sinh[(1-\alpha)\ln(\omega\tau_c)]}{g(\alpha,\omega,\tau_c)}\right), \tag{7}$$

$$\chi''(\omega) = \frac{\chi_T - \chi_{\mathrm{ad}}}{2}\left(\frac{\cos\left(\frac{1}{2}\alpha\pi\right)}{g(\alpha,\omega,\tau_c)}\right), \tag{8}$$

where $g(\alpha,\omega,\tau_c) = \sin\left(\frac{1}{2}\alpha\pi\right) + \cosh[(1-\alpha)\ln(\omega\tau_c)]$. For the purpose of fitting experimental data to the Eqs. (7) and (8) one often plots χ'' vs χ' (Cole-Cole diagram), corresponding to the equation

$$\chi''(\chi') = -\frac{\chi_T - \chi_{\mathrm{ad}}}{2\tan\left[\frac{1}{2}\pi(1-\alpha)\right]} + \left[\left(\frac{\chi_T - \chi_{\mathrm{ad}}}{2}\right)^2 + \left(\frac{\chi_T - \chi_{ad}}{2\tan\left[\frac{1}{2}\pi(1-\alpha)\right]}\right)^2 - \left(\chi' - \frac{\chi_T + \chi_{\mathrm{ad}}}{2}\right)^2\right]^{1/2}. \tag{9}$$

This yields χ_T, χ_{ad}, and α, and permits τ_c to be extracted from a fit of Eqs. (7) and (8) with χ_T, χ_{ad}, and α set to the values determined in the fitting of the Cole-Cole equation [Eq. (9)]. Equation (9) represents a circular arc of size $(1-\alpha)\pi$ cutting the χ' axis at $\chi' = \chi_{\mathrm{ad}}$ and $\chi' = \chi_T$. At the maximum of χ'': $\omega\tau_c = 1$.

IV. RESULTS AND ANALYSIS

A. dc measurements

In Figs. 1(a) and 1(b) the field dependencies of the magnetization $M(H)$ for SBN61: Ce and SBN61: Cr at low temperatures are shown. The indicated lines correspond to the fit of the data measured at different temperatures to Eq. (1) (Brillouin function). Thereby the g-value and the number of moles $N_{Cr^{3+},Ce^{3+}}$ of Ce^{3+} or Cr^{3+} atoms contributing to the signal, are refined. The angular momenta J are fixed to the ground state values $J = 5/2$ for SBN61: Ce and $J = 3/2$ for SBN61: Cr, respectively. The simultaneous fitting of Eq. (1)

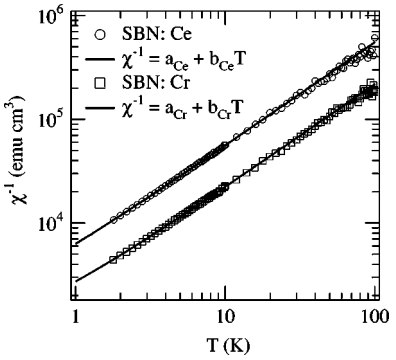

FIG. 2. Inverse static susceptibility for SBN61: Ce, Cr. Fit-parameters: $a_{Ce}=8(2)\cdot 10^2$ mol$\cdot$cm^{-3}, $b_{Ce}=5.5(1)\cdot 10^3$ mol$\cdot$cm^{-3} K^{-1}, $a_{Cr}=5.5(5)\cdot 10^2$ mol$\cdot$cm^{-3}, and $b_{Cr}=2.2(1)\cdot 10^3$ mol$\cdot$cm^{-3} K^{-1}.

to the magnetization curves at four or five different temperatures ensures that the g-values and the number density n can be extracted independently, since the g-value is mostly determined by the curvature while n is determined by the saturation value of the magnetization curve. For SBN61: Cr the fit yields $g=1.88(2)$, which is slightly smaller than the typical g-values for Cr^{3+} reported in the literature ($g=1.91$–1.98). This may be due to demagnetization effects at the crystal surface or deviations due to a misalignment of the crystal axis with respect to the applied magnetic field, which were not taken into account. Furthermore the number density is determined as $n_{Cr^{3+}}=1.51(6)\cdot 10^{20}$ cm^{-3}. For SBN61: Ce one obtains $g=1.16(1)$ and $n_{Ce^{3+}}=0.72(1)\cdot 10^{20}$ cm^{-3}. The Landé g-value for Ce^{3+} is $g_J=6/7$, but since the crystal field splits the ground state into the doublets $|\pm 1/2\rangle (g=6/7)$, $|\pm 3/2\rangle (g=18/7)$, $|\pm 5/2\rangle (g=30/7)$, the effective g-value may differ from g_J, depending on the position and population of the doublets. One may therefore compare the obtained g-value with those measured by EPR,[7] where an orthorhombic g-tensor $\{g_{[100]-\phi}, g_{[010]-\phi}, g_{[001]}\}=\{0.89, 3.55, 0.54\}$ with principal axes lying in the c-plane, tilted with respect to the a- and b-axes by $\phi=21.1°$, and along the c-axis, was found. Using

$$g^2 = \cos^2\,\theta \cdot g^2_{[100]-\phi} + \sin^2\,\theta \cdot g^2_{[010]-\phi} \tag{10}$$

one finds $\theta=12.5°$, or an angle of 8.6° between applied magnetic field and a-axis of the crystal, which is in the range of the accuracy of the crystal orientation in the PPMS.

The static susceptibility follows the Curie-Weiss law in both compounds as shown in Fig. 2. From the fit to the inverse susceptibility $\chi^{-1}(T)$ one can determine the number density for the same valence state from the slope b of the graph in Fig. 2

$$n = N_A b^{-1} C^{-1}, \quad C = 0.125 g^2 J(J+1)\ \text{cm}^3\ \text{K mol}^{-1} \tag{11}$$

when using the g-values determined from the field dependence of the magnetization and the J values of the corresponding ground states. The resulting values are shown in Table I together with the averages calculated from the fits for the magnetization and the susceptibility.

TABLE I. Parameters obtained from dc-measurements with number densities given in units of 10^{20}(cm^{-3}) from (Fig. 1) and (Fig. 2), and X=Cr or Ce. The averaged number densities is denoted by $\overline{n}_{X^{3+}}$.

	J	g^*	$n^{M(H)}_{X^{3+}}$	$n^{\chi(T)}_{X^{3+}}$	$\overline{n}_{X^{3+}}$	θ_c(K)
Ce	$\frac{5}{2}$	1.16(1)	0.72(1)	0.74(1)	0.73(1)	−0.14(4)
Cr	$\frac{3}{2}$	1.88(2)	1.51(6)	1.65(8)	1.58(8)	−0.25(3)

The paramagnetic Curie temperatures are deduced from the abscissa a of the inverse susceptibility

$$\theta_c = -naCN_A^{-1}, \quad C = 0.125 g^2 J(J+1)\ \text{cm}^3\ \text{K mol}^{-1}. \tag{12}$$

One obtains $\theta_c=-0.14(4)$ K for SBN61: Ce and $\theta_c=-0.25(3)$ K for SBN61: Cr, respectively. θ_c is considered here only as a fit parameter, since several physical phenomena can contribute to a deviation from the pure Curie law. The parameters resulting from the dc measurements are summarized in Table I together with the averaged number density $\overline{n}_{X^{3+}}$ from both measurements.

B. ac-measurements

ac measurements on both samples reveal that the response of SBN61: Ce is frequency dependent whereas that of SBN61: Cr is not. The frequency dependence of the dynamic susceptibility of SBN61: Ce is therefore studied as a function of temperature and applied magnetic field. Figure 3 shows as an example the frequency dependence of SBN61: Ce as a function of temperature at $H=100$ Oe and as a function of magnetic field for $T=2.3$ K. The maximum in the imaginary part $\chi''(\omega)$ of the dynamic susceptibility shifts to higher fre-

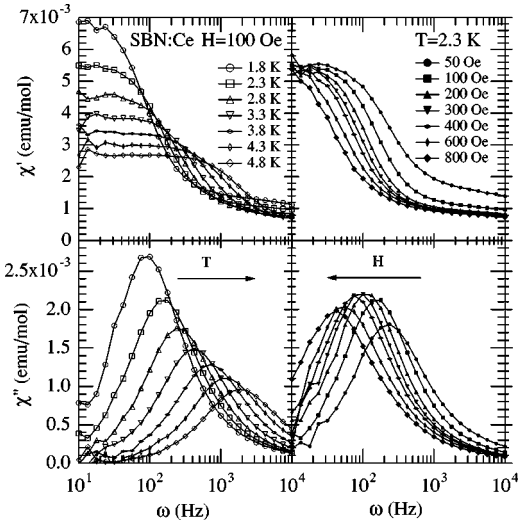

FIG. 3. Frequency dependence of the dynamic susceptibility in SBN61: Ce as a function of magnetic field and temperature. Lines are a guide to the eye.

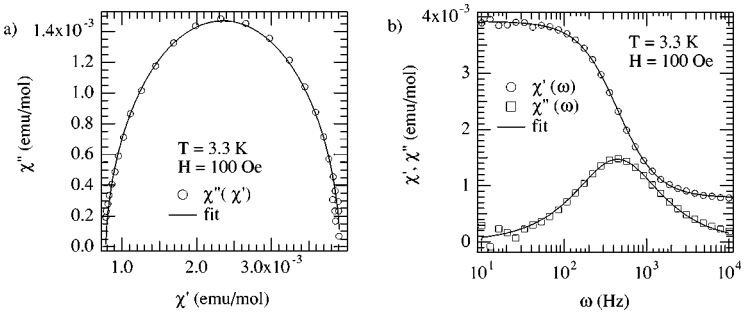

FIG. 4. (a) Fit to the Cole-Cole Eq. (9) of the dynamic susceptibility in SBN61: Ce at $T=3.3$ K and $H=100$ Oe. The fit yields $\chi_T=3.92(5)\cdot10^{-3}$ emu/mol, $\chi_{ad}=7.82(4)\cdot10^{-4}$ emu/mol, and $\alpha=0.042(5)$. (b) Fits to the Cole-Cole Eq. (7) and (8) of the dynamic susceptibility in SBN61: Ce at $T=3.3$ K and $H=100$ Oe. The fit yields the mean relaxation time $\tau_c=2.25(2)\cdot10^{-3}$ s.

quencies with increasing temperature and decreases in size. On the other hand the maximum shifts to lower frequencies with increasing magnetic field. The data can be fitted with the Cole-Cole Eq. (9), indicating that a distribution of relaxation times is involved in the relaxation mechanism. In Fig. 4(a) such a fit is shown for $T=2.3$ K and $H=100$ Oe. From this fit the adiabatic and isothermal susceptibility as well as the parameter α are obtained. In this case α is close to zero, indicating that the relaxation time distribution is narrow and the system is close to a Debye relaxor. The values determined for χ_{ad}, χ_T, and α are then used as input for the fit of the mean relaxation time τ_c, obtained from a fit of Eqs. (7) and (8) to the curves $\chi'(\omega)$ and $\chi''(\omega)$, as indicated in Fig. 4(b). Performing this fit procedure for every temperature measured at the field $H=100$ Oe, one obtains the temperature dependence of the relaxation time presented in Fig. 5. Fitting Eq. (4) to this curve, one obtains the contributions of the different mechanisms involved in the relaxation process, determined by the constants A_2, B_2, and C_2 and the level splitting Δ'. Performing this procedure for all measured fields (from 50 Oe to 2000 Oe) the field dependence of the single processes results. The level splitting $\Delta'=20.6(4)$ K (corresponding to 1.77(4) meV) shows no observable field

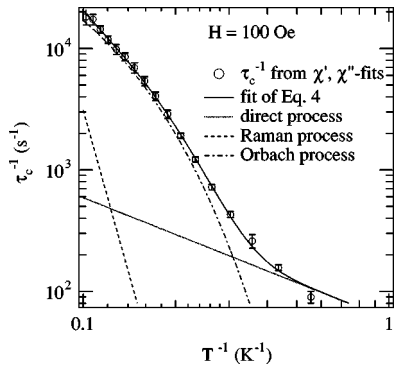

FIG. 5. Temperature dependence of the mean relaxation time τ_c at $H=100$ Oe in SBN61: Ce. The fit was performed using Eq. (4) and yields $A_2=5.9(3)\cdot10^{-7}$ s^{-1} Oe^{-4} K^{-1}, $B_2=3(3)\cdot10^{-6}$ s^{-1} K^{-9}, $C_2=1.5(2)\cdot10^{5}$ s^{-1}, and $\Delta'=21.5(7)$K. The dashed lines indicate the contributions of the single processes involved in the relaxation.

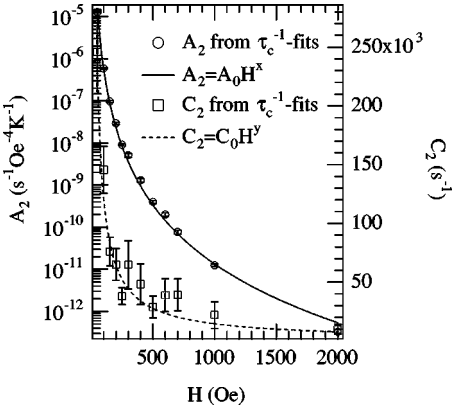

FIG. 6. Field dependencies of the fitted parameters A_2 and C_2. The lines correspond to power laws fitted to the data. Fit-parameters: $A_0=1.1(1)\cdot10^{3}$ s^{-1} Oe^{-4} K^{-1}, $x=-4.64(2)$, $C_0=9(4)\cdot10^{6}$ s^{-1}, and $y=-0.92(9)$ (see Table II).

dependence since a field-induced level splitting is small for field strengths up to 2000 Oe. The constant $B_2=7.5(5)\cdot10^{-6}$ s^{-1} K^{-9} associated with the Raman processes is also field independent.

The constants A_2 and C_2 on the other hand exhibit a field dependence as illustrated in Fig. 6. Fitting a power law for the field dependence of the Orbach process

$$C_2 = C_0 H^y \tag{13}$$

one finds $y=-0.92(9)$ and $C_0=9(4)\cdot10^{6}$ s^{-1} and therefore $C_2\sim H^{-1}$. This can be understood when looking at the series expansion of the last term in Eq. (4) which yields $1/\tau\sim k_BT/\Delta'$. If $\Delta'\sim H$ one obtains the observed H^{-1}-dependence. Orbach processes can occur only in crystals where the electronic energy levels are lying within the phonon spectrum, i.e., where the condition

$$g\mu_B H < \Delta' < k_B\theta_D \tag{14}$$

is valid. For magnetic fields up to 2000 Oe $g\mu_BH/k_B<0.5$ K, so that the left condition of Eq. (14) is always fulfilled. The Debye temperature θ_D of SBN61: Ce is approximately 300 K, as was checked by measuring the heat capacity of two SBN61 samples doped with different amounts of cerium (0.4 wt.% and 0.8 wt.% CeO_2 in the melt). In the case of the direct process one would not expect any additional field dependence since a H^4-dependence was already taken into account in the fit by Eq. (4). Nevertheless the parameter A_2 ranges over many orders of magnitude (10^{-5}–10^{-13} s^{-1} Oe^{-4} K^{-1}) in the measured field range up to 2000 Oe. Fitting a power law to the field dependence of A_2

$$A_2 = A_0 H^x \tag{15}$$

one obtains $A_0=1.1(1)\cdot10^{3}$ s^{-1} Oe^{-4} K^{-1} and $x=-4.64(2)$. Comparing the observed $H^{-4.64}$ dependence with the expected H^4 dependence one obtains a final field dependence of the direct process of $H^{-0.64}$. One has to be careful in interpreting this result, since the experimentally available temperature range, where the direct process is dominating, is rather limited (see Fig. 5). An explanation of the unexpected

TABLE II. Relaxation parameters for SBN61: Ce obtained from ac-measurements.

Δ'(K)	A_0 (s^{-1} Oe^{-4} K^{-1})	x	B_2 (s^{-1} K^{-9})	C_0 (s^{-1})	y
20.6(4)	$1.1(1)\cdot 10^3$	−4.64(2)	$7.5(5)\cdot 10^{-6}$	$9(4)\cdot 10^6$	−0.92(9)

field dependence of the direct process may be the appearance of the *phonon bottleneck* at low temperatures (see e.g., Ref. 15).

The exact crystal field-induced levels for low symmetry are not known and temperatures below 1.8 K cannot be reached with the PPMS used. Furthermore the precise positions of the Ce^{3+} ions in the SBN lattice are not known up to now, only the symmetry is known to be C_1 from EPR measurements.[7] In addition we have to take into account that Ce^{3+} has, compared to other trivalent rare earths, the largest $\langle r^2\rangle$ value and in all rare earths the 5*s* and 5*p* shells lie well outside the 4*f* shells, thus any distortion of these cells can play an important role in crystal field effects.[16] Therefore the following discussion of $\Delta'=20.6(4)$ K in SBN: Ce should prove only the plausibility of our result. Thus we did not perform a detailed theoretical analysis based on crystal field calculations like Ruby *et al.*[17] have done for Ce^{3+} in lanthanum magnesium nitrate, Scott and Jeffries[15] for Ce^{3+} in ethyl sulfate, or Hellwege *et al.*[18] for the mixed system $La_{1-x}Ce_xCl_3$. In all cases the crystal field (C_{3v}, C_{3h}, C_{3h}-symmetry) splits the $4f^1\ ^2F_{5/2}$ ground state multiplet into the three doublets at 0 K, 34 K, 200 K, 0 K, 5.7 K, 186 K, and 0 K, 54 K, 158 K, respectively. The energy values of 34 K, 5.7 K, and 54 K of the first excited level correspond to $\Delta'=20.6(4)$ K at least within the order of magnitude. We mention that very recently three narrow absorption lines corresponding to $^2F_{5/2}\rightarrow{}^2F_{7/2}$ transitions have been observed and deconvoluted, but no energy difference equal to Δ' have been observed for all three transitions starting from the same ground state level.[19] The parameters obtained for the spin-lattice relaxation in SBN61: Ce are summarized in Table II.

V. CONCLUSIONS

Measurements of the magnetization $M(H)$ and the static susceptibility $\chi(T)$ offer the possibility to determine the number density of paramagnetic ions $n_{X^{3+}}$ doped into crystals. The results of both methods agree well within the experimental errors for doping with X=Ce,Cr in SBN, as illustrated in Table I.

These results are complementary to our previous investigations concerning the number density of dopants in SBN using instrumental neutron activation analysis (INAA) and x-ray fluorescence (XRF),[6,8] where the total number density n_X of the dopants was determined. Thus, the comparison between the values determined from the combination of INAA/XRF with the ones from magnetization and static susceptibility provides insight into the number density of dopants with valence state different to 3+.

It is obvious from Table III that the total amount of Ce determined with INAA deviates from $\overline{n}_{Ce^{3+}}$. This indicates that a considerable amount of Ce is present, which does not contribute to the magnetization, but is well detected by the INAA technique. A very probable candidate is Ce^{4+}. We therefore determine $n_{Ce^{4+}}$ via $n_{Ce^{4+}}+n_{Ce^{3+}}=n_{Ce}^{INAA}$ and obtain $n_{Ce^{4+}}=1.19(9)\cdot 10^{20}$ cm^{-3}.

On the other hand the agreement between the data for Cr points to a primarily build-in of Cr in the valence state Cr^{3+}, i.e., the number density of Cr^{4+} is small. Here we get $n_{Cr^{4+}}=0.06(8)\cdot 10^{20}$ cm^{-3}.

The determination of the number density of dopants in different valence states is especially of importance for photorefractive applications. In SBN Ce and Cr act as photorefractive centers so that the valence state is changed from 3 + to 4+ by light-induced excitation of free charge carriers or from 4+ to 3+ by trapping, respectively. The knowledge of the respective number densities $n_{X^{3+}}$ and $n_{X^{4+}}$, respectively, allows to understand and describe the kinetics and steady state properties of the resulting space charge fields, which modulate the refractive index via the electro-optic effect. However, we have to stress that the values determined by the magnetization and static susceptibility should not be mixed up with the number densities $\tilde{n}_{X^{3+}}, \tilde{n}_{X^{4+}}$ deduced from photorefractive measurements, e.g., via the determination of the effective trap density $N_{eff}=\tilde{n}_{X^{3+}}\cdot\tilde{n}_{X^{4+}}/(\tilde{n}_{X^{3+}}+\tilde{n}_{X^{4+}})$ valid for SBN. The effective trap density involves various properties like cross section, type of charge transport mechanism and all kinds of valence states of photorefractive centers, i.e., it takes into account the number of charge carriers effectively involved in the photorefractive effect. In contrast, the number densities determined by the magnetization and static susceptibility represents the number of all available free charge carriers for photorefraction so that the relations $n_{X^{3+}}\geqslant\tilde{n}_{X^{3+}}$ and $n_{X^{4+}}\geqslant\tilde{n}_{X^{4+}}$hold.

The dynamic susceptibility of SBN61: Ce shows a distinct frequency dependence. Analysis of the data reveals that a distribution of relaxation times is involved in the spin-lattice relaxation process. This can be explained by the fact that Ce^{3+} occupies a Sr-position (off-center) in the SBN lattice,[7,20] which is disordered due to the incommensurate modulation. Therefore every Ce^{3+} ion sees a slightly different environment. This leads to a different level splitting and influences therefore the relaxation time distribution. From Fig. 5 it can be seen that the Orbach process dominates the relaxation behavior of SBN61: Ce in the temperature range 3–10 K. At the lowest temperatures the direct process pro-

TABLE III. Number densities in units of $10^{20}(cm^{-3})$ for Cr- and Ce-doped SBN.

	$\overline{n}_{X^{3+}}$	n_X^{INAA}	n_X^{INAA/XRF_8}
Ce	0.73(1)	1.92(8)	
Cr	1.58(8)		1.64(8)

vides the fastest relaxation times. Raman processes play only a minor role in this system over the measured temperature range 1.8–10 K. The dynamic susceptibility of SBN61: Cr does not exhibit a frequency dependence in the range $10–10^4$ Hz. Cr occupies a Nb-position inside the oxygen octahedra in the SBN lattice. This site is much less disordered than the Sr-sites, as has been shown by x-ray and neutron diffraction.[21,22] Furthermore the different energy level splitting due to the crystalline electric field in Cr influences also the relaxation behavior. From the susceptibility measurements on these two samples one cannot decide, whether the different positions inside the SBN lattice or the different type of the dopant is responsible for the different magnetic behavior.

ACKNOWLEDGMENTS

Financial support by the Swiss National Science Foundation (Grant No. 21-57084.99), the Deutsche Forschungsgemeinschaft (WO618/3-4) and the European Community (INTAS, Grant No. 0173) is gratefully acknowledged.

*Electronic address: dominik.schaniel@uni-koeln.de

[1] J. Ford, J. Ma, Y. Fainman, S. Lee, Y. Taketomi, D. Bize, and R. Neurgaonkar, J. Opt. Soc. Am. A **9**, 1183 (1992).
[2] P. Yeh and A. Chiou, Opt. Lett. **12**, 138 (1987).
[3] G. Wood, W. Clark III, M. Miller, E. Sharp, G. Salamo, and R. Neurgaonkar, IEEE J. Quantum Electron. **23**, 2126 (1987).
[4] R. Neurgaonkar, W. Cory, J. Oliver, M. Ewbank, and W. Hall, Opt. Eng. **26**, 392 (1987).
[5] T. Chernaya, B. Maksimov, I. Verin, L. Ivleva, and V. Simonov, Crystallogr. Rep. **42**, 375 (1997).
[6] T. Woike, G. Weckwerth, H. Palme, and R. Pankrath, Solid State Commun. **102**, 743 (1997).
[7] J. Wingbermühle, M. Meyer, O. Schirmer, R. Pankrath, and R. Kremer, J. Phys.: Condens. Matter **12**, 4277 (2000).
[8] T. Woike, U. Dörfler, L. Tsankov, G. Weckwerth, D. Wolf, M. Wöhlecke, T. Granzow, R. Pankrath, M. Imlau, and W. Kleemann, Appl. Phys. B: Lasers Opt. **B72**, 661 (2001).
[9] T. Volk, T. Woike, U. Dörfler, R. Pankrath, L. Ivleva, and M. Wöhlecke, Ferroelectrics **203**, 457 (1997).
[10] P. Dutta, A. Manivannan, M. S. Seehra, P. M. Adekkanattu, and J. A. Guin, Catal. Lett. **94**, 181 (2004).
[11] K. Buse, Appl. Phys. B: Lasers Opt. **B64**, 391 (1997).
[12] R. Carlin and A. van Duyneveldt, *Magnetic Properties of Transition Metal Compounds* (Springer Verlag, Berlin, 1977).
[13] K.-H. Hellwege, *Einführung in die Festkörperphysik* (Springer Verlag, Berlin, 1976).
[14] K. Cole and R. Cole, J. Chem. Phys. **9**, 341 (1941).
[15] P. Scott and C. Jeffries, Phys. Rev. **127**, 32 (1962).
[16] A. Freeman and R. Watson, Phys. Rev. **127**, 2058 (1962).
[17] R. Ruby, H. Benoit, and C. Jeffries, Phys. Rev. **127**, 51 (1962).
[18] K. Hellwege, E. Orlich, and G. Schaack, Phys. Kondens. Mater. **4**, 196 (1965).
[19] R. Demirbilek, A. B. Kutsenko, R. Pankrath, and S. E. Kapphan, Ferroelec. **303**, 775 (2004).
[20] T. Chernaya, T. Volk, B. Maksimov, M. Blomberg, L. Ivleva, I. Verin, and V. Simonov, Crystallogr. Rep. **48**, 933 (2003).
[21] T. Woike, V. Petříček, M. Dušek, N. Hansen, P. Fertey, C. Lecomte, A. Arakcheeva, G. Chapuis, M. Imlau, and R. Pankrath, Acta Crystallogr., Sect. B: Struct. Sci. **B59**, 28 (2003).
[22] D. Schaniel, J. Schefer, V. Petříček, M. Imlau, R. Pankrath, T. Granzow, and T. Woike, Appl. Phys. A: Mater. Sci. Process. **A74**, 963 (2002).